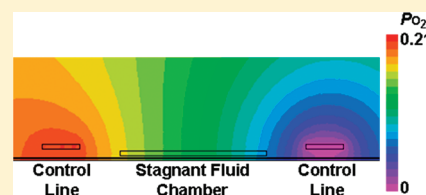


Regulating Oxygen Levels in a Microfluidic Device

Peter C. Thomas,^{†,‡} Srinivasa R. Raghavan,[§] and Samuel P. Forry^{*,†}[†]Biochemical Science Division, National Institute of Standards and Technology, Gaithersburg, Maryland 20899, United States[‡]Fischell Department of Bioengineering, University of Maryland, College Park, Maryland 20742, United States[§]Department of Chemical and Biomolecular Engineering, University of Maryland, College Park, Maryland 20742, United States

Supporting Information

ABSTRACT: Microfluidic devices made from poly(dimethylsiloxane) (PDMS) are gas permeable and have been used to provide accurate on-chip oxygen regulation. However, pervaporation in PDMS devices can rapidly lead to dramatic changes in solution osmotic pressure. In the present study, we demonstrate a new method for on-chip oxygen control using pre-equilibrated aqueous solutions in gas-control channels to regulate the oxygen content in stagnant microfluidic test chambers. An off-chip gas exchanger is used to equilibrate each control solution prior to entering the chip. Using this strategy, problems due to pervaporation are considerably reduced. An integrated PDMS-based oxygen sensor allows accurate real-time measurements of the oxygen within the microfluidic chamber. The measurements were found to be consistent with predictions from finite-element modeling.



In vitro studies have demonstrated that oxygen levels affect cellular growth,¹ enzyme expression,² and stem cell differentiation.^{3,4} In addition, naturally occurring oxygen gradients, a result of mass-transfer limitations, have been suggested to regulate proper tissue function,⁵ influence cell development,⁴ and elicit the onset of angiogenesis.⁶ As such, new approaches to regulating in vitro cell culture oxygen levels could improve our understanding of oxygen-dependent cellular behavior. While mammalian cells in tissue are found at an oxygen partial pressure (P_{O_2}) of 3% to 9% oxygen ($P_{O_2} = 0.03$ atm – 0.09 atm),⁷ conventional cell culture incubators, in contrast, are typically maintained at the ambient level of 21% oxygen ($P_{O_2} = 0.21$ atm). To reduce the oxygen level during in vitro cell culture, various hypoxic chambers have been developed. However, the time required for culture medium to reach equilibrium and the lack of ability to generate oxygen gradients limit the scope of application for such chambers.⁸

Gas-permeable, poly(dimethylsiloxane) (PDMS)-based microfluidic devices offer alternative approaches to existing methods of oxygen regulation.^{9–15} With the utilization of passive diffusion, external oxygen gas pumped through a control channel equilibrates through PDMS with the dissolved oxygen in adjacent fluidic channels, thereby achieving oxygen regulation on the device. Given the small distance between channels and the high permeability of oxygen through PDMS,¹⁶ equilibrium can be achieved quickly (within seconds).^{12,13} In addition, oxygen gradients can be generated using different oxygen–nitrogen gas mixtures across a device.¹³ While this method of oxygen control is an improvement, the current design allows significant pervaporation of water through the PDMS.¹⁷ In mammalian cultures where the temperature is held at 37 °C, the aqueous liquid within a fluidic chamber can quickly evaporate and pass through the PDMS, resulting in dramatically increased osmolarity of the liquid.¹⁷ This issue is potentially

exacerbated when gas-filled control channels are placed in close proximity to fluidic channels for gas control. To circumvent this problem, mammalian cells are often cultured in the device under continuous flow conditions. However, this precludes culturing cells that are sensitive to shear stress and limits the potential applicability of microfluidic methods.

In the current study, we demonstrate a new approach for regulating oxygen on a microfluidic chip. In contrast to previous methods, pre-equilibrated aqueous solutions of different dissolved oxygen compositions were pumped through gas control channels to modulate the oxygen levels in neighboring stagnant chambers. Equilibrium through the bulk PDMS gave rapid control of the dissolved oxygen composition. To monitor the changing oxygen levels within the fluidic chamber in real-time and continuously, we integrated an oxygen sensor previously developed in our lab into the PDMS device.¹⁸ Additionally, the aqueous solutions in the control lines replaced water lost to the environment via pervaporation.¹⁹ While different techniques have separately addressed oxygen regulation and pervaporation control, we demonstrate for the first time the ability to simultaneously regulate the oxygen level and also reduce evaporation using water-filled control lines.

EXPERIMENTAL SECTION

PDMS-based multilayer microfluidic devices were fabricated using photolithography and soft lithography techniques.²⁰ The current design has a single fluidic line that widens into a chamber, positioned between two control lines (Figure 1). Pneumatic valves placed upstream and downstream from the chamber

Received: August 30, 2011

Accepted: October 13, 2011

Published: October 13, 2011

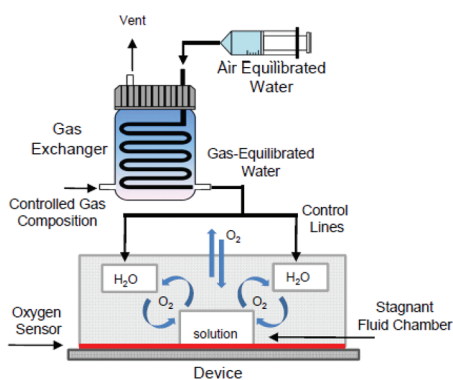


Figure 1. Schematic of microfluidic device setup for on-chip oxygen regulation. Water was pumped through the gas exchanger where the P_{O_2} in the liquid is reduced via equilibration with the controlled gas composition. This solution then enters the microfluidic control lines flanking the fluid chamber of the device. An oxygen sensor integrated into the floor of the device (red) measures changes of P_{O_2} as dissolved oxygen in the control lines diffuse through the PDMS and into the adjacent fluid chamber. Schematic not drawn to scale.

regulated the liquid flow. Control lines and the fluid chamber were $250\ \mu\text{m}$ and $1000\ \mu\text{m}$ wide, respectively. Two designs were tested: in one, the horizontal distance between the fluid chamber and the control line was $200\ \mu\text{m}$ and in the other this distance was $80\ \mu\text{m}$. The vertical distance between the two was $\sim 10\ \mu\text{m}$ in all cases. All channels were $30\ \mu\text{m}$ tall. Before introduction on-chip, the gas partial pressure in control solutions was modulated using a gas exchanger constructed using gas-permeable Teflon AF tubing with i.d. = $600\ \mu\text{m}$ and o.d. = $800\ \mu\text{m}$ (Biogeneral Inc., San Diego, CA).²¹

An oxygen-sensing PDMS film, based on the porphyrin dye, Pt(II) meso-tetrakis(pentafluorophenyl) porphine (PtTFPP, Frontier Scientific Inc., Logan, Utah), was prepared and calibrated as described previously.¹⁸ Briefly, PtTFPP was dissolved in PDMS (Slygard 184; Dow-Corning, Midland, MI) and spin coated onto a microscope slide. Separate layers of Teflon AF (Dow Chemical) and PDMS were sequentially spin-coated and cured. The total sensor thickness was $\sim 24\ \mu\text{m}$. This oxygen sensor was integrated with the microfluidic device through plasma bonding. Calibration of the on-chip sensor was accomplished by exposing the device to controlled levels of oxygen gas. Emission intensity from the sensor was captured and used to generate a calibration curve. Because the thin-film sensor covered the entire surface, spatial variations in the oxygen level could be monitored across the whole device.

Pervaporation experiments were performed at a temperature of $37\ ^\circ\text{C}$ to mimic cell culture conditions. A $10\ \mu\text{M}$ solution of dextran conjugated with rhodamine (molecular weight $\sim 70\ 000$; Sigma, St. Louis, MO) was used as a marker for changes in the solute concentration. A steady-state 2D finite element model was developed using FlexPDE software based on the device and channel geometry (Supporting Information; Figure S-2).

RESULTS AND DISCUSSION

Regulation of the oxygen level on-chip was accomplished using an off-chip gas exchanger. Water, pumped through the gas exchanger, first equilibrated with the oxygen level there. The high oxygen permeability of Teflon tubing (990 barrer, from manufacturer Web site) and the short diffusion distance (tubing wall thickness $\sim 100\ \mu\text{m}$) allowed rapid equilibration

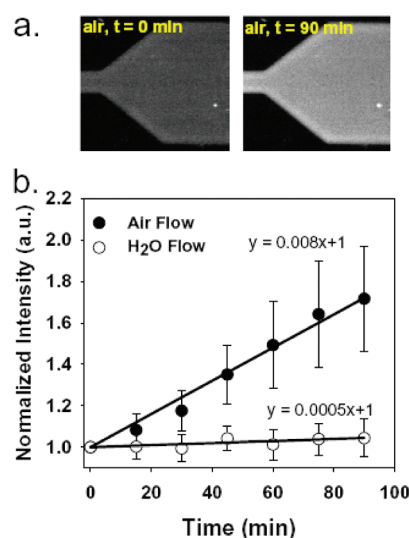


Figure 2. Effects of water pervaporation during device operation. Fluorescent intensity of dextran conjugated rhodamine solution increased due to pervaporation when humidified air was pumped through the control lines (a). On-chip regulation of gas partial pressure using water-filled control lines (○) mitigated the effects of pervaporation as compared to humidified gas flow (●) (b). The pervaporation rate when flowing humidified air was calculated ($0.248\ \text{nL}/\text{min}$) from the fluorescence doubling time (2 h) and the device geometry. In each case, the mean intensity value across the fluid chamber was normalized at $t = 0$; error bars indicate the standard deviation of triplicate measurements. Solid lines show linear regressions for each system with the fitted equations.

with the P_{O_2} set point. At a flow rate of $700\ \mu\text{L}/\text{min}$ (residence time of the liquid in the gas exchanger was $\sim 100\ \text{s}$), the oxygen level in the liquid had fully equilibrated by the time the liquid left the gas exchanger. Equilibration was determined by monitoring the oxygen levels in the liquid as it exits the gas exchanger (data not shown).

Previously, we had developed a PDMS-based, thin-film oxygen sensor using the phosphorescent dye, PtTFPP.¹⁸ Here, we integrated this sensor film into the floor of the microfluidic device through plasma bonding. The emission intensity from the film is quenched in the presence of oxygen, and the relationship between the two is given by the linear Stern–Volmer equation:²²

$$\frac{I_0}{I} = 1 + K_{SV} \times P_{O_2} \quad (1)$$

where I_0 is the phosphorescence intensity of the sensor under pure N_2 ($P_{O_2} = 0\ \text{atm}$), I is the quenched intensity at elevated oxygen levels, K_{SV} is the Stern–Volmer constant, and P_{O_2} is the partial pressure of oxygen. The calibration of the sensor was performed via pixel-by-pixel analysis where each pixel was assigned a separate Stern–Volmer constant. The K_{SV} determined for the on-chip sensor ($517 \pm 100\ \text{atm}$) matched previous bulk sensors,¹⁸ indicating that the sensitivity of the measurement was not affected by the assembled microfluidic device (Supporting Information; Figure S-1). As liquid carrying lower dissolved oxygen was introduced on-chip, the oxygen level within the device equilibrated by diffusion and was monitored in real time by the oxygen sensor.

Given the small volume of liquid within the microfluidic device, pervaporation can rapidly alter solute concentrations, potentially affecting a cell culture experiment. To monitor the changes in solute concentration during operation, emission

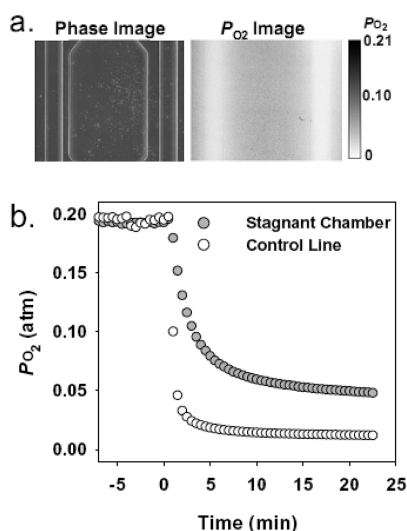


Figure 3. Rapid P_{O_2} response on-chip. Images of the microfluidic device via phase contrast (left) and P_{O_2} (right) show the position of the fluid chamber with two flanking control lines (a). Initially, air equilibrated with water flows through the control lines, and the P_{O_2} in the stagnant fluid chamber remains at 0.2 atm. When the gas exchanger is filled with N_2 ($P_{O_2} = 0$ atm; $t = 0$ min), oxygen levels in the control line reached steady state within 2 min, matching closely the residence time of liquid in the gas exchanger (b). Steady state oxygen level in the fluid chamber is achieved in 8.5 min. The P_{O_2} image in part a is taken from $t = 20$ min in part b.

intensity of dextran conjugated with rhodamine was monitored continuously in the fluidic channel while a downstream valve was closed. When warm humidified gas was pumped through the control lines, an increase in rhodamine fluorescence with time was observed in the stagnant fluid chamber (Figure 2a). This was consistent with fresh rhodamine solution entering the chamber to replace liquid lost through pervaporation. From the steady increase in solute concentration, an osmolality doubling time of 2 h was calculated. For the geometry of the system, this gave a pervaporation rate of ~ 0.25 nL/min (Supporting Information). In contrast, pervaporation effects were mitigated when warm water was pumped through the control lines, and no increases in rhodamine intensity were observed (Figure 2b). The effect of water-filled control lines here was analogous to the incorporation of a water reservoir specifically designed to prevent pervaporation.²³

By reducing the P_{O_2} in the control lines, oxygen levels can be reduced within the fluid chamber. The thin film sensor integrated into the floor of the microfluidic system allowed spatial variations in P_{O_2} across the entire device to be monitored (Figure 3a). Previous devices demonstrated oxygen regulation by directly overlapping the gas and fluid channels.^{12,13} Adler et al. demonstrated the ability to generate different oxygen gradients by designing multiple control lines directly above a liquid line.¹³ Equilibration times in these systems varied depending on the distance between channels and were typically on the order of seconds. The current device minimizes potential light scattering and optical interference by incorporating control lines adjacent to the fluidic chamber.

With the current system, steady state P_{O_2} levels in the control lines were achieved in 2 min after air was switched to N_2 in the gas exchanger (Figure 3b). The oxygen level in the fluid chamber equilibrated more slowly and reached a steady state in 8 min.

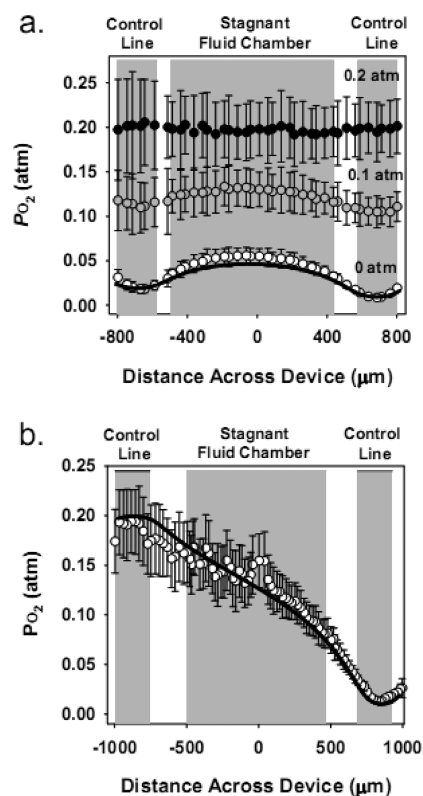


Figure 4. P_{O_2} equilibration. The oxygen level across the device equilibrated with P_{O_2} set points in the aqueous solutions pumped through the control lines (a). By flowing air-equilibrated and N_2 -equilibrated water on opposite sides of the stagnant fluid chamber, an oxygen gradient was formed across the device (b). Oxygen measurements from the sensor match the results of finite element simulations (black line). Gray regions in the graphs indicate the location of the two control lines flanking the stagnant fluid chamber (middle). Data points represent the mean P_{O_2} value; the error bars depict the standard error.

A P_{O_2} across the whole device of 0.03 atm–0.05 atm was achieved with this design (Figure 4a), providing a physiologically relevant oxygen environment. (P_{O_2} levels significantly lower than 0.03 atm, as required for hypoxic studies, could not be attained with the current device design.) A 2D finite element model was developed based on the steady state diffusion equation:

$$D_{O_2} \frac{\partial^2 C}{\partial x^2} = 0 \quad (2)$$

where D_{O_2} is the diffusion coefficient of oxygen in PDMS, c is the oxygen partial pressure, and x is the distance. Using the geometry of the device cross section, simulations were performed to determine the on-chip oxygen levels as solutions with different dissolved oxygen content were pumped through the control lines (Supporting Information; Figure S-2). The height of the device was the only adjustable parameter for the model. The simulation showed good agreement with experimental data (Figure 4a), indicating oxygen transport in the device could be accounted for with a simple 2D diffusion model from eq 2. The current system allows rapid control of on-chip oxygen levels within physiological ranges, and the oxygen sensor provides real-time monitoring. In addition, the diffusive simulation model allows alternative geometries to be quickly evaluated prior to fabrication.

With air-equilibrated and N₂-equilibrated water pumped into opposing control lines, an oxygen gradient was formed across the device (Figure 4b). The finite element model again showed excellent agreement with experimental data.

CONCLUSIONS

Precise regulation of the oxygen level is critical in many applications (e.g., understanding how oxygen affects cell function and response). Gas permeable PDMS-based microfluidic devices offer the advantage of fast and precise control of the oxygen level; however, continuous operation can result in pervaporation and dramatic changes in osmotic pressure. Here, instead of pumping gases directly through the device, water with varying dissolved oxygen concentrations was pumped through the control lines to achieve regulation of the oxygen level. The use of water-filled control lines significantly mitigated pervaporation effects. Using this strategy, we demonstrated that physiological oxygen levels (P_{O_2} of 0.03 atm–0.05 atm) could be maintained on-chip, or oxygen gradients could be generated. The integration of an oxygen sensor into the floor of the microfluidic device allowed real time, in situ monitoring of the oxygen partial pressure. The current strategy allows the oxygen level to be monitored across the entire device, thus providing a tool for understanding how changes in oxygen level propagate throughout the entire microfluidic system. Experimental P_{O_2} measurements showed excellent agreement with finite element simulations. Compared to previous strategies which have addressed these issues separately, we have developed a microfluidic system that provides on-chip oxygen control while simultaneously mitigating pervaporation. Future experiments will examine cell-based culture systems using the current approach for controlling oxygen partial pressure.

ASSOCIATED CONTENT

S Supporting Information. Additional information as noted in text. This material is available free of charge via the Internet at <http://pubs.acs.org>.

AUTHOR INFORMATION

Corresponding Author

*E-mail: sam.forry@nist.gov. Phone: (301) 975-5246.

REFERENCES

- (1) Parrinello, S.; Samper, E.; Krtolica, A.; Goldstein, J.; Melov, S.; Campisi, J. *Nat. Cell Biol.* **2003**, *5*, 741–747.
- (2) Camp, J. P.; Capitano, A. T. *Biotechnol. Prog.* **2007**, *23*, 1485–1491.
- (3) Keith, B.; Simon, M. C. *Cell* **2007**, *129*, 465–472.
- (4) Simon, M. C.; Keith, B. *Nat. Rev. Mol. Cell Biol.* **2008**, *9*, 285–296.
- (5) Jungermann, K.; Kietzmann, T. *Hepatology* **2000**, *31*, 255–260.
- (6) Carmeliet, P.; Jain, R. K. *Nature* **2000**, *407*, 249–257.
- (7) Sahaf, B.; Atkuri, K.; Heydari, K.; Malipatlolla, M.; Rappaport, J.; Regulier, E.; Herzenberg, L. A.; Herzenberg, L. A. *Proc. Natl. Acad. Sci. U.S.A.* **2008**, *105*, 5111–5116.
- (8) Wright, W. E.; Shay, J. W. *Nat. Protoc.* **2006**, *1*, 2088–2090.
- (9) Vollmer, A. P.; Probst, R. F.; Gilbert, R.; Thorsen, T. *Lab Chip* **2005**, *5*, 1059–1066.
- (10) Park, J.; Bansal, T.; Pinelis, M.; Maharbiz, M. M. *Lab Chip* **2006**, *6*, 611–622.
- (11) Lam, R. H. W.; Kim, M. C.; Thorsen, T. *Anal. Chem.* **2009**, *81*, 5918–5924.

(12) Polinkovsky, M.; Gutierrez, E.; Levchenko, A.; Groisman, A. *Lab Chip* **2009**, *9*, 1073–1084.

(13) Adler, M.; Polinkovsky, M.; Gutierrez, E.; Groisman, A. *Lab Chip* **2010**, *10*, 388–391.

(14) Higgins, J. M.; Eddington, D. T.; Bhatia, S. N.; Mahadevan, L. *Proc. Natl. Acad. Sci. U.S.A.* **2007**, *104*, 20496–20500.

(15) Lo, J. F.; Sinkala, E.; Eddington, D. T. *Lab Chip* **2010**, *10*, 2394–2401.

(16) Merkel, T. C.; Bondar, V. I.; Nagai, K.; Freeman, B. D.; Pinnau, I. *J. Polym. Sci., Part B: Polym. Phys.* **2000**, *38*, 415–434.

(17) Heo, Y. S.; Cabrera, L. M.; Song, J. W.; Futai, N.; Tung, Y. C.; Smith, G. D.; Takayama, S. *Anal. Chem.* **2007**, *79*, 1126–1134.

(18) Thomas, P. C.; Halter, M.; Tona, A.; Raghavan, S. R.; Plant, A. L.; Forry, S. P. *Anal. Chem.* **2009**, *81*, 9239–9246.

(19) Forry, S. P.; Locascio, L. E. *Lab Chip*, **2011**, DOI: 10.1039/C1LC20505F.

(20) Unger, M. A.; Chou, H. P.; Thorsen, T.; Scherer, A.; Quake, S. R. *Science* **2000**, *288*, 113–116.

(21) Certain commercial products are identified in order to adequately specify the experimental procedure; this does not imply endorsement or recommendation by NIST.

(22) Lakowicz, J. R. *Principles of Fluorescence Spectroscopy*; Plenum Press: New York, 1983

(23) Song, J. W.; Gu, W.; Futai, N.; Warner, K. A.; Nor, J. E.; Takayama, S. *Anal. Chem.* **2005**, *77*, 3993–3999.

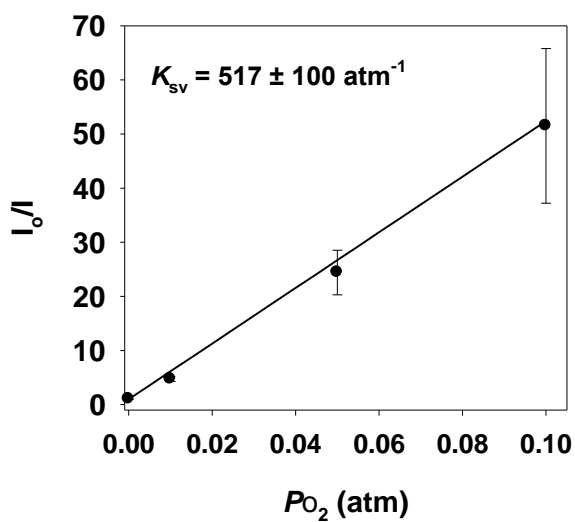
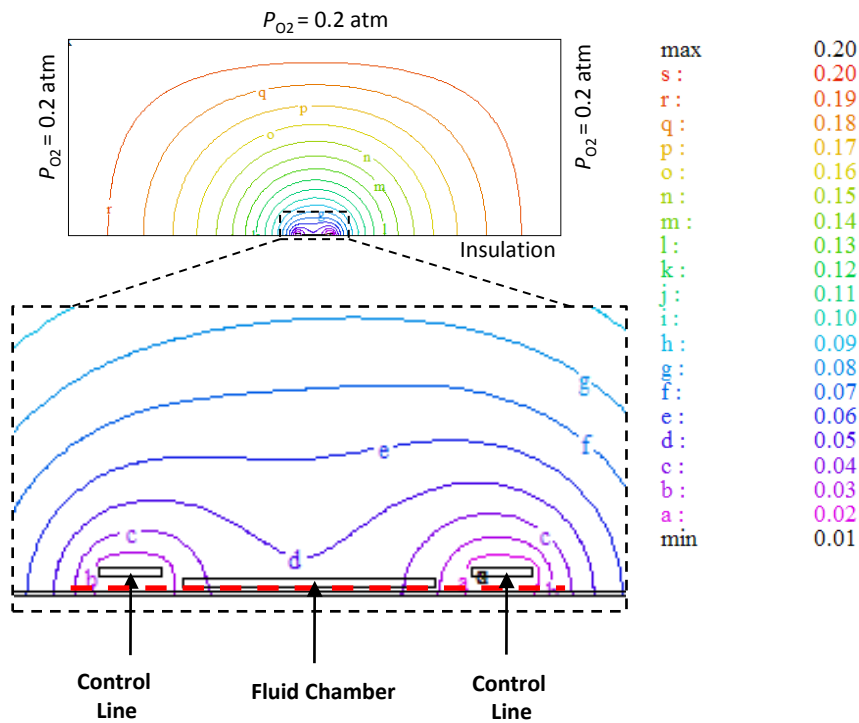


Figure S-1 On-chip P_{O_2} sensor calibration. The response of the integrated oxygen sensor follows the Stern-Volmer equation. Data points represents the mean value of all the pixels (360000 pixels) and error bars indicate their standard deviation.

a.



b.

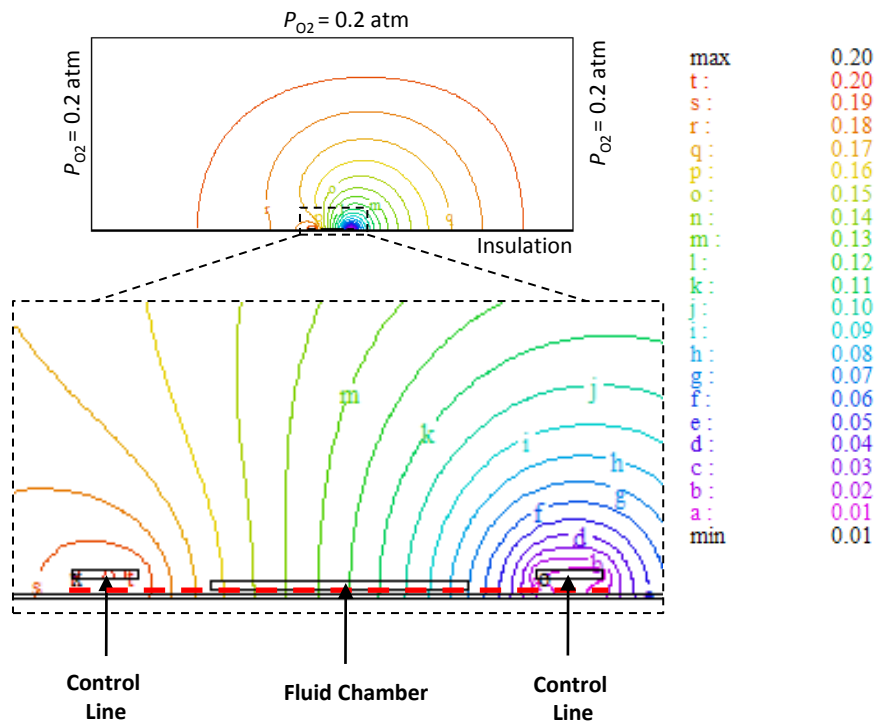


Figure S-2 Two dimensional steady state numerical simulation of oxygen levels in a microfluidic device. The simulated geometry was 21 mm wide x 8 mm high, with boundary conditions of $P_{O_2} = 0.2 \text{ atm}$ on three sides exposed and an oxygen impermeable bottom. The legend provides the P_{O_2} (in atm) of the contour lines. When the boundary conditions of the two control lines were set at $P_{O_2} = 0.02 \text{ atm}$ (left) and 0.012 atm (right) to match the sensor measurements, oxygen level on-chip was reduced (a).

The inset shows the two control lines flanking the fluid chamber and the location of simulated oxygen measurement (red dashed line). To simulate oxygen gradient, P_{O_2} of control lines were set at 0.2 atm (left) and 0.008 atm (right) based on the experimental measurements (b). The input parameters for the diffusion of oxygen in PDMS, Teflon AF, and water are $3.3 \cdot 10^{-5}$ cm²/s, $2 \cdot 10^{-6}$ cm²/s, and $4 \cdot 10^{-5}$ cm²/s, respectively. The current simulation consists of 60536 nodes.

ESI Pervaporation calculation

The total volume V of the liquid is the volume of the cell chamber:

$$V = 1000 \mu\text{m} \times 1000 \mu\text{m} \times 30 \mu\text{m} = 3 \times 10^{-5} \text{ cm}^3$$

The volume of the chamber is assumed constant, therefore the slope from Figure 2b, is the rate of the fold change for the volume. The rate of pervaporation is determined from total volume multiplied by the rate of fold change:

$$3 \times 10^{-5} \text{ cm}^3 \times 0.0083 \text{ min}^{-1} = 2.47 \times 10^{-7} \text{ cm}^3/\text{min}$$